A single dumbbell falling under gravity in a cellular flow field

2003 J. Phys. A: Math. Gen. 36 4291

(http://iopscience.iop.org/0305-4470/36/15/306)

INSTITUTE OF PHYSICS PUBLISHING JOURNAL OF PHYSICS A: MATHEMATICAL AND GENERAL

J. Phys. A: Math. Gen. **36** (2003) 4291–4306 PII: S0305-4470(03)57845-3

A single dumbbell falling under gravity in a cellular flow field

M F Piva and S Gabbanelli

Grupo de Medios Porosos, Facultad de Ingeniería, Universitas de Buenos Aires, Paso Colón 850 (1063), Buenos Aires, Argentina

E-mail: mpiva@fi.uba.ar

Received 2 January 2003, in final form 14 February 2003
Published 3 April 2003
Online at stacks.iop.org/JPhysA/36/4291

Abstract

We study the motion of a single polymer chain settling under gravity in an ensemble of periodic, cellular flow fields, which are steady in time. The molecule is an elastic dumbbell composed of two beads connected by a nonbendable Hookean spring. Each bead is subject to a Stokes drag and a Brownian force from the flow. In the absence of particle inertia, the molecule settles out at a rate which depends on three parameters: the particle velocity in a fluid at rest, V_g, the spring constant, B, and the diffusion coefficient, D. We investigate the dependence of the molecule settling velocity on B, for fixed V_g and D. It is found that this velocity strongly depends on B and it has a minimum value less than V_g. We also find that the molecule is temporarily trapped at fixed points for certain values of the parameters. We analyse one fixed point in detail and conclude that its stability is the main factor which contributes to slowing down the settling process.

PACS numbers: 92.10.We, 82.35.Lr, 05.60.−K

1. Introduction

In this paper, we investigate numerically the motion of a single polymer chain in the presence of gravity as it moves through a convective pattern of rolls. This study is motivated by previous studies related to the motion of polymer chains in elongational or rotational flows [1, 2], in which it was stated that a polymer chain approaching a stagnant point in pure elongational flows tends to elongate while its residence time, t_{res}, diverges. In contrast, a polymer chain moving in pure rotational flow has a tendency to rotate without deformation.

Several flows of practical interest consist of a mixture of both rotational and elongational components and the resulting transport properties of polymer chains will be affected by the particular structure of the velocity field.

Thus, in the case of a polymer chain settling under gravity in the presence of a convective flow it may be speculated that its settling motion will slow down in the vicinity of a stagnant point. As a consequence, the average settling velocity of such a molecule could be smaller than that in a fluid at rest. This reduction in the terminal velocity will in general depend on the size of the molecule in view of its relation with the molecule relaxation time. Therefore, it appears that sedimentation in a convective pattern of rolls may induce polymer segregation by size and that is the practical importance of this study.

In a general context, the motion of particles settling under gravity in a given flow field is a subject not only intricate but interesting as well. This problem has captured the attention of investigators in many areas of engineering, meteorology and oceanography. Similar problems may be found in the settling of particles in colloidal suspensions [3], in the motion of bubbles in liquid reservoirs [4], in the dynamical behaviour of heavy markers [5] and in several other flows of engineering interest.

The simplest problem involving sedimenting particles is that of noninteracting heavy particles drifting down in a quiescent fluid [6]. Assuming that the particles start at rest, they are accelerated downwards by the action of gravity but they asymptotically reach a stationary state in which the driving force (gravity) is balanced by the dissipative force (viscous drag). The particle velocity is then constant, its value depending on several parameters such as the particle size and mass, the fluid viscosity and the value of the acceleration due to gravity.

The average settling velocity may be strongly modified if the particle settles in the presence of flow structures such as eddies or convection patterns. For example, in flow regions with upward velocities the gravity force may be balanced by the viscous drag and particles could be suspended indefinitely, remaining trapped at an equilibrium point or moving in closed orbits. On the other hand, if a heavy particle moves in flow regions with downward velocities, gravity and drag forces act in the same direction leading to an enhanced settling process with a settling velocity larger than in the quiescent fluid.

A simple flow field which reproduces the main properties of a convective pattern of rolls is given by the stream function [9]:

$$\psi(x, y) = (U_o/k) \sin kx \sin ky \tag{1}$$

which consists of a periodic array of counterrotating eddies with a characteristic velocity, U_o, and the periodicity of the cell, $2\pi/k$. This flow field has been used extensively to represent the main features of particle motion in flows with recirculating zones such as those in thermal convection when a layer of fluid is heated from below or in Taylor–Couette instability where a periodic pattern of toroidal vortices appear for some angular velocities of the internal cylinder [7].

In this flow field, the falling of single spherical particles was studied first by Stommel [8] and later by Maxey [9, 10]. In an early approach Stommel showed that the vertical motion of a particle without inertia may be strongly influenced by the flow field given by equation (1). Indeed, he showed that particles may remain suspended indefinitely, depending on the ratio between their terminal velocity in a fluid at rest and the characteristic fluid velocity U_o. In this case, the convective flow forces the particles to move upwards in regions of strong upflow. Then, a sort of dynamical equilibrium between gravity and the Stokes drag is reached and the particle moves in closed orbits in a single cell.

In the same flow field, Maxey [10] considered the settling of heavy particles for which the inertia and added mass term are not negligible. He showed that particles with non-negligible inertia are never suspended in the flow field and they settled more rapidly than in a fluid at rest. Also he shows that particles have a tendency to cumulate in isolated asymptotic trajectories.

In this work, we are interested in the motion of a simple polymer chain as it falls under gravity in the flow field given by equation (1). Two different types of behaviour may be expected: elongation and slowing down of the molecule as it approaches points with coordinates $(kx, ky) = (m\pi, n\pi)$, where the flow is purely elongational, and rotation without deformation around points $(kx, ky) = ((m + 1/2)\pi, (n + 1/2)\pi)$, where the flow is purely rotational. The goal is to determine the interaction between the internal structure of the molecule and the flow field and how it modifies the rate at which the molecule settles under gravity.

A polymer molecule is usually represented as a long chain of elemental units called monomers. Several models have been proposed to describe the behaviour of polymer chains in a given solvent. One of the most widely used is the Rouse model which assumes that a linear polymer chain can be represented as a set of N beads joined by springs [11]. The simplest example of a Rouse chain, called the 'elastic dumbbell', corresponds to $N = 2$. This model, a crude but useful representation of a polymer molecule, has been successful in describing many of the rheological properties of real polymers, such as orientability and stretchability or migration effects in shear flows [12].

To achieve a simple model of the dynamical equation of the dumbbell, we consider that the flow field is not affected by the presence of the molecule. In addition, we neglect molecule–molecule interactions considering low concentration of particles. The fluid force on each bead, considered to be small enough so that we can neglect couples due to the local shear, was calculated ignoring the presence of the other bead. Fluid forces acting on each bead are the viscous frictional force, or Stokes drag, and the Brownian force provided by the solvent molecules. In this first approach particle inertia will be neglected.

More details of the dumbbell model, together with the complete set of dynamical equations, are presented in section 2. We will show that the dynamics of the molecule is governed by three dimensionless parameters: the spring stiffness, B, the diffusion coefficient, D, and the Stokes velocity of a single particle, V_g.

In section 3, we present some examples of dumbbell trajectories. The dependence of the average settling velocities, $\langle V \rangle$, on B, V_g and D is studied, and the conditions for which the molecule settles out slower or faster than in a fluid at rest are analysed.

The main features of the results are discussed in section 4. We show that the decrease in the average settling velocity is due to the existence of equilibrium points at which the dumbbells may be trapped for a certain time. Finally, concluding remarks are given in section 5.

2. Equations for dumbbell motion

In figure 1, we show a schematic view of the dumbbell molecule immersed in a fluid. Two beads of radius a are connected at their centres by a Hookean spring of stiffness B'. The hydrodynamic force on one of the beads due to its motion relative to the fluid is the Stokes drag: $6\pi a\mu(\mathbf{u} - \mathbf{v})$, where $\mathbf{u}$ is the fluid velocity at the centre of the bead, $\mathbf{v}$ is the velocity of the bead and μ the fluid viscosity.

Following the classical formulation of the dumbbell model [11], we assume that the solvent exerts on the beads a Brownian force given by $\sqrt{2D'}\eta$ where η describes a normalized white noise process for which $\langle \eta(t) \rangle = 0$ and D' is the noise density (or the diffusion coefficient) for the single bead in bulk fluid. Finally, we also consider that a bead under gravity in a fluid at rest settles out with a terminal velocity V_g.

The sum of all the forces is set to zero in order to derive the noninertial equations of motion for the molecule. For each bead labelled 1 and 2 we obtain

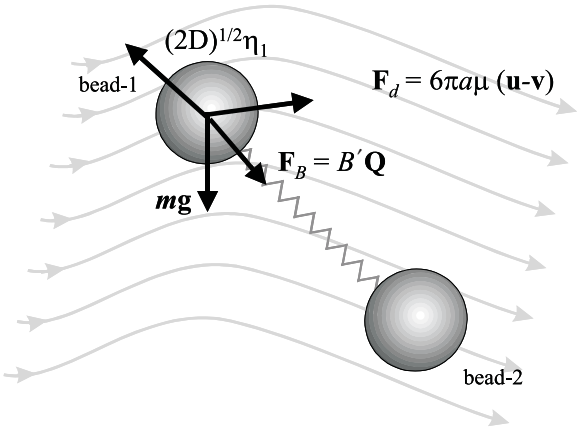

Figure 1. Schematic view of the elastic dumbbell in the (x, y)-plane of the flow. Arrows indicate the instantaneous balance of forces on one of the spheres.

$$\mathbf{v}_1 = \mathbf{u}(\mathbf{r}_1) + \frac{B'}{6\pi a\mu}\mathbf{Q} + \sqrt{2D'}\eta_1 + \frac{m\mathbf{g}}{6\pi a\mu} \tag{2}$$

$$\mathbf{v}_2 = \mathbf{u}(\mathbf{r}_2) - \frac{B'}{6\pi a\mu}\mathbf{Q} + \sqrt{2D'}\eta_2 + \frac{m\mathbf{g}}{6\pi a\mu} \tag{3}$$

where $\mathbf{Q} = \mathbf{r}_2 - \mathbf{r}_1$ is the distance between beads, m the bead mass and $\mathbf{g}$ the gravitational acceleration constant. The flow velocity, $\mathbf{u}$, is derived from equation (1) which corresponds to a periodic arrangement of eddies with velocity components given by

$$u_x = \frac{\partial\psi}{\partial y} = U_o \sin kx \cos ky \tag{4a}$$

$$u_y = -\frac{\partial\psi}{\partial x} = -U_o \cos kx \sin ky. \tag{4b}$$

From here on we use U_o and $1/k$ as the characteristic scales to nondimensionalize the equations of motion. The corresponding nondimensional equations, assuming that gravity is aligned with the positive y-axis, are

$$\begin{aligned} v_{x1} &= \sin x_1 \cos y_1 + B(x_2 - x_1) + \sqrt{2D}\eta_{1x} \\ v_{y1} &= -\cos x_1 \sin y_1 + B(y_2 - y_1) + \sqrt{2D}\eta_{1y} + V_g \\ v_{x2} &= \sin x_2 \cos y_2 - B(x_2 - x_1) + \sqrt{2D}\eta_{2x} \\ v_{y1} &= -\cos x_2 \sin y_2 - B(y_2 - y_1) + \sqrt{2D}\eta_{2y} + V_g \end{aligned} \tag{5}$$

where B and D are the nondimensional spring constant and diffusion coefficient, respectively, and $V_g = mg/6\pi a\mu U_o$ the single-particle settling velocity in a fluid at rest.

Before describing the settling dynamics of the dumbbell in the general case, let us consider two limit situations for which equations (5) are considerably simplified.

The first case corresponds to $B = 0$. Setting the spring constant to zero implies that beads are disconnected and, therefore, the velocity of any of them is described by the following equations:

$$v_x = \sin x \cos y + \sqrt{2D}\eta_x \qquad v_y = -\cos x \sin y + \sqrt{2D}\eta_y + V_g. \tag{6}$$

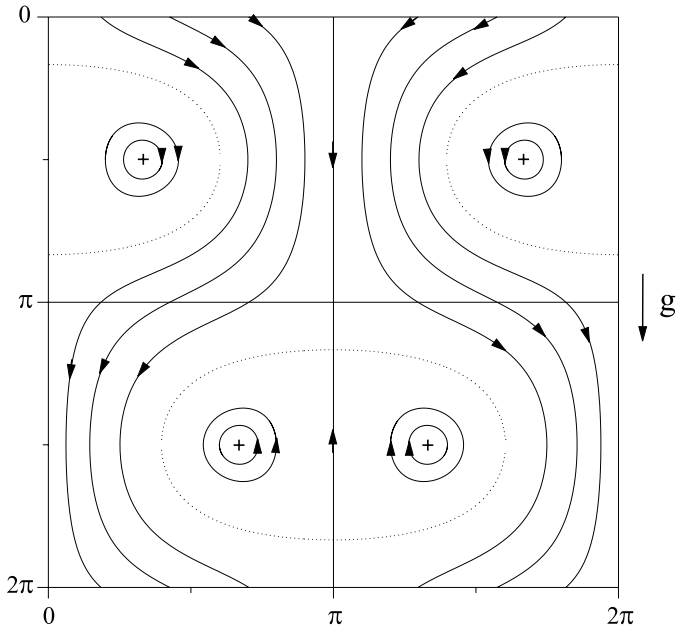

Figure 2. Trajectories of single particles settling under gravity in the cellular flow field for $V_g = 0.5$: +, static equilibrium point; ——, particle path; - - - -, bounding trajectory for the trapping region. Arrows indicate the circulation in each cell.

It can be seen that the settling dynamics of a single particle is governed by the sum of the local velocity of the fluid, the Brownian contribution and the settling velocity in a fluid at rest. This problem, with the diffusion term set equal to zero, was first studied by Stommel [8] and later revisited by Maxey *et al* [9]. In view of its relevance for the present work, we summarize below the most important results obtained by these authors.

Stommel shows that particle suspension occurs only for values of V_g in the range $0 < V_g < 1$. From equations (6) it can be seen that if $V_g > 1$ then the fluid velocity never exceeds V_g and the particle velocity is positive at all times and thus particles settle out. Figure 2 shows some sample particle trajectories for $V_g = 0.5$. Suspended particles move around closed paths encircling an equilibrium point. The trapping region is bounded by a particle path (shown with a dashed line) that joins the cell boundary. Outside this region particles settle out.

Maxey pointed out that the fraction of the particles in trapping regions will be suspended indefinitely but the rest of the particles will settle out with velocities larger than V_g.

When the diffusion term $\sqrt{D}\eta$ is considered in equations (6), the single-particle dynamics acquires a nondeterministic character. The motion does not occur in closed or open paths, in contrast, the particle moves in irregular paths because of the Brownian contribution to the particle velocity. The general picture that emerges is that of a particle that spends part of the time suspended in the trapping regions and part of the time in zones with a positive settling velocity larger than V_g. In this condition, the distinction between suspended and sedimenting particles disappears and all the particles settle out with an average settling velocity equal to V_g.

The second limiting case we will analyse is $B \to \infty$. In this limit the spring term in equation (5) becomes dominant and therefore, the drag is not enough to maintain the beads

separated and the molecule collapses. It is convenient to rewrite the equations in terms of $\mathbf{R} = (X, Y) = (\mathbf{r}_2 + \mathbf{r}_1)/2$, $\mathbf{V} = (V_x, V_y) = (\mathbf{v}_2 + \mathbf{v}_1)/2$, the position and velocity of the centre of mass, respectively, as

$$V_x = \frac{u_x(\mathbf{r}_2) + u_x(\mathbf{r}_1)}{2} + \sqrt{D}\eta_x \qquad V_y = \frac{u_y(\mathbf{r}_2) + u_y(\mathbf{r}_1)}{2} + \sqrt{D}\eta_y + V_g. \tag{7}$$

The collapse of the molecule implies that $\mathbf{r}_2 \to \mathbf{r}_1 = \mathbf{R}$ and equations (7) result in

$$V_x = \sin X \cos Y + \sqrt{D}\eta_x \qquad V_y = -\sin Y \cos X + \sqrt{D}\eta_y + V_g. \tag{8}$$

These equations are equivalent to those obtained for $B = 0$ except for the diffusion term divided by 2. Thus, when $B \to \infty$ the motion of the centre of mass of the dumbbell is similar to that of a single particle. Therefore, in the presence of diffusion, the average velocity of the centre of mass must be equal to V_g.

In conclusion, at the limiting values of B the molecule behaves as a single particle and therefore, deviations from this behaviour may be only expected for intermediate values of this parameter. Let us now consider briefly the general case: $0 < B < \infty$. For these values of B, equations (5) show the effect of the spring term. If the beads are close to one another the contribution of the spring term to the bead velocity is negligible and the total velocity is mainly due to the flow and the fluid settling velocity, V_g. In contrast, if the beads are separated by a distance comparable to the cell length, π, this term dominates and the molecule evolves in order to minimize its length. The first phenomenon occurs when the dumbbell moves near the centre of a cell where the molecule experiences low stresses. The second one occurs near the separatrix between two cells where the stresses are large.

As a consequence, for fixed D and V_g, the settling motion of the molecule through the cellular flow is controlled by the spring constant, a situation which will lead to a settling dynamics very different from that encountered for single rigid particles of the type studied by Maxey *et al* [10].

3. Numerical results

It is expected that the dynamics of the molecule will be affected by the value of the spring constant and that the average settling velocity of the centre of mass of the molecule, $\langle V_y \rangle$, shows some dependence on this parameter. In order to study this dependence, we calculate some trajectories of the molecule for given values of the parameters B, V_g and D.

Equations (5) were numerically integrated by using a second-order Runge–Kutta method with a step size $\Delta t = 0.01$. Each bead of the molecule was located at a random initial position in the square $[0, 2\pi] \times [0, 2\pi]$. Then, the position of the centre of mass and its instantaneous velocity components $V_x(t)$ and $V_y(t)$ were calculated. For a large number of molecules, N, the average settling velocity of the centre of mass, $\langle V \rangle = \langle V_y \rangle$, was obtained from the time average:

$$\langle V \rangle = \frac{1}{N} \sum_{i=1}^{N} \frac{1}{T} \int_0^T V_y^i(t)\, \mathrm{d}t \tag{9}$$

where i indexes the molecule number and T is a large end-time that depends on the parameters B, D and V_g. It was considered that $\langle V \rangle$ has reached its stationary value if $\langle \delta V \rangle < 10^{-5} \langle V \rangle$ where $\langle \delta V \rangle$ is the statistical deviation of V_y from its average. In all cases stationary results were obtained for $T > 3 \times 10^5$.

In the first series of simulations, we studied the effect of the spring constant B, for fixed values of the parameters D and V_g. Figure 3 shows some examples of molecule paths in the

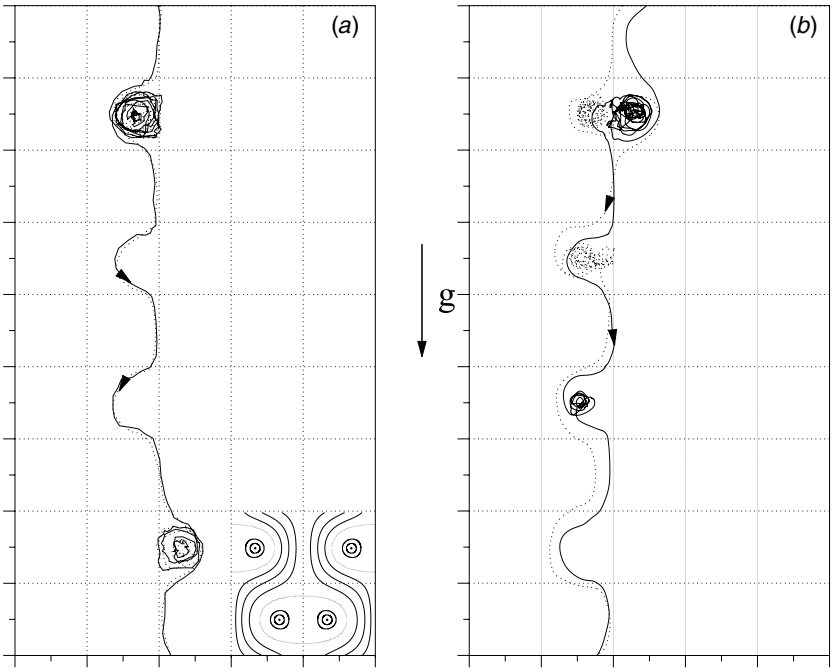

Figure 3. Dumbbell trajectories for different spring constants. Paths of each bead of the dumbbell were plotted separately with full lines and dotted lines, respectively. Values of the parameters B, D and V_g are (a) $B = 0.7$, $D = 0.01$, $V_g = 0.5$ and (b) $B = 0.06$, $D = 0.01$, $V_g = 0.5$. Beginning at the upper left corner the cells were numbered ij, i and j denoting rows and columns, respectively. The inserted plot in the lower right corner is the single-bead velocity streamline.

cellular flow field, in which the trajectory of each bead was plotted separately. The parameters used in the simulations are $V_g = 0.5$, $D = 0.01$, and two different values of the spring constant: $B = 0.7$ and $B = 0.06$. In the figure, each cell is considered as the ij element of a matrix. The inset, at the lower right corner, shows the single-bead velocity streamlines as shown in figure 2.

It can be seen that the bead paths in figure 3(a) are closer than in figure 3(b). In both paths shown in figure 3(a) the beads remain for some time in cell 2-2: they are trapped in the corresponding trapping region of the single-bead velocity field. Due to stochastic jumps the molecule is able to leave this region and continues to settle following open streamlines of the single-bead velocity field. When the molecule reaches the cell 8-3 with a settling velocity larger than V_g, it is trapped and the settling process is again interrupted. The sequence of fast settling motion followed by trapping events is repeated all along its path. The main feature of the molecule motion is determined by $V_y(t)$, which averaged over a long time T, according to equation (9), remains close to V_g. Accordingly, the molecule length remains much smaller than the cell size. This effect is shown in figure 4(a), where the probability distribution of molecule lengths for this set of parameters is plotted.

Figure 3(b) shows a very different behaviour. It is clear that the beads move in separate paths. After they leave from the cells numbered 1-2 and 2-3, they are trapped in cells 2-2 and 2-3. Then, the beads settle out but later they are trapped together in the cell 4-2. Afterwards, it can be seen that while one of the beads (dotted line) still remains in the cell 4-2 the other evolves to the cell 6-2. Note that in this condition the molecule length is close to 2π. They

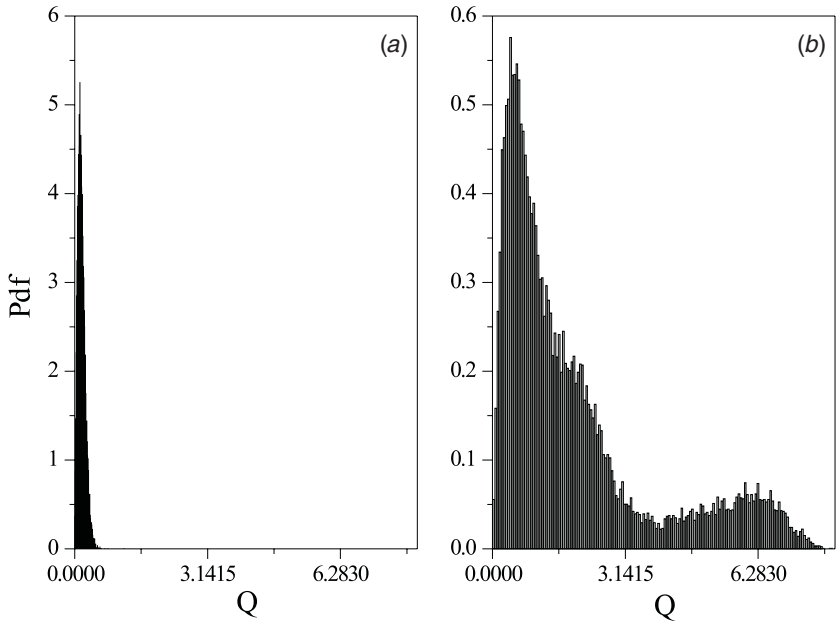

Figure 4. Dumbbell length distribution along a path for two sets of parameters: (*a*) $B = 0.7$, $D = 0.01$, $V_g = 0.5$ and (*b*) $B = 0.06$, $D = 0.01$, $V_g = 0.5$.

remain in this asymmetric situation until the bead in cell 4-2 leaves this location and settles out until it reaches the other trapped bead. After this sequence, the beads settle out in separated but almost parallel paths. In this example, the average settling velocity was found to be considerably smaller than that in a fluid at rest, V_g. In agreement, figure 4(*b*) shows that the probability distribution of molecule lengths spreads over distances larger than the cell size and it exhibits local maxima. It will be shown in the next section that the reason for this behaviour is the existence of a stable fixed point for values of the spring constant smaller than a critical one. This fixed point occurs at some specific spatial locations in the cellular flow field where the gravity force on each bead is balanced by the sum of the drag and the spring forces. In such locations, if the Brownian force on each bead is small enough, the dumbbell remains for a long time near the attractive basin of the fixed point until it is finally swept away by the downflow. The slowing down of the dumbbell motion in the proximity of a fixed point contributes thus to diminishing the average settling velocity to values smaller than V_g.

Figure 5 shows the variations in average settling velocity $\langle V \rangle$ as the spring constant increases from $B = 0$ to $B = 1$, and for $V_g = 0.5$ and for different values of D.

For $D = 0.01$ and $D = 0.005$ there is a significant reduction in the average settling velocity near $B = 0.08$ which is more pronounced for decreasing values of D. The minimum value of $\langle V \rangle$ slightly depends on B. All curves approach asymptotically to $V_g = 0.5$ as B increases.

It is interesting to remark that $\langle V \rangle$ remains close to V_g even for values of the spring constant as small as 0.5, indicating that the molecule behaves as a single particle while in section 2 it was assumed that the molecule collapse occurs for $B \to \infty$.

Figure 5 also shows the effect of the diffusion coefficient D on the dumbbell dynamics. It was found that for some values of the diffusion coefficient the average settling velocity goes to zero. This situation occurs in figure 5 for $D = 0.001$ where it can be seen that $\langle V \rangle = 0$

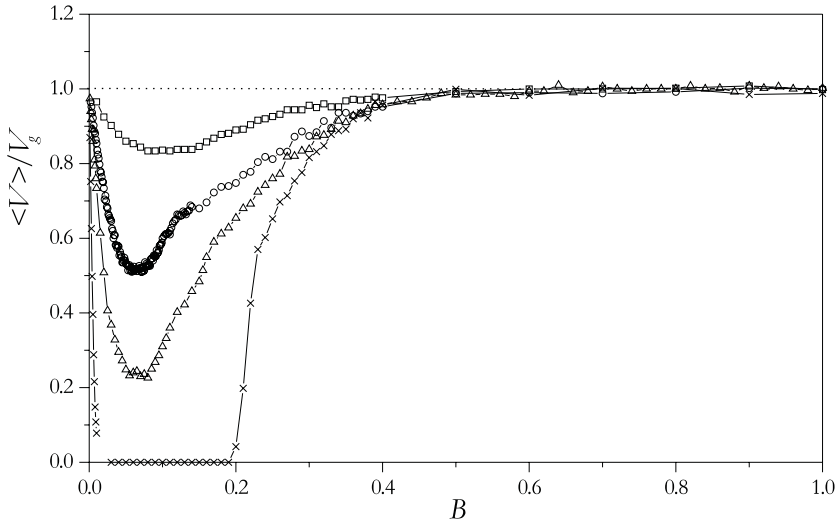

Figure 5. Normalized dumbbell average settling velocity against B for $V_g = 0.5$: □, $D = 0.05$; ○, $D = 0.01$; △, $D = 0.005$; ×, $D = 0.001$.

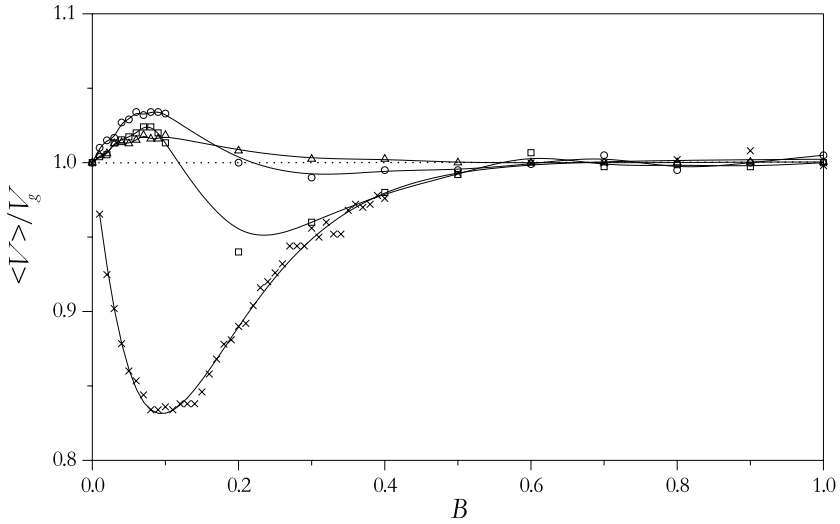

Figure 6. Normalized dumbbell average settling velocity against B for $D = 0.05$: △, $V_g = 1.25$; ○, $V_g = 1$; □, $V_g = 0.75$; ×, $V_g = 0.5$.

for B in the range $(0.01, 0.2)$. This behaviour is connected with the existence of fixed points as was mentioned in a previous paragraph. When the diffusion coefficient D is sufficiently small, the Brownian force is not enough to drive the dumbbell out of the influence zone of the fixed point and the average settling velocity goes to zero.

The influence of the still fluid settling velocity, V_g, is shown in figure 6. It can be seen that the average settling velocity $\langle V \rangle$ tends to V_g as the spring constant increases. This behaviour is observed for all the values of V_g investigated, either smaller or larger than $V_g = 1$, indicating that for large B the molecule behaves as a single particle. The most remarkable fact is the

maximum of $\langle V \rangle$ that occurs for some values of $V_g > 0.5$. This maximum implies that the molecule settles out faster than V_g, a phenomenon related to the ability of the molecule to stretch and explore regions of downward flow, which will be described in more detail in the following section.

4. Equilibrium points and stability

In the previous section, it was suggested that values of $\langle V \rangle$ smaller than V_g or zero occur due to the existence of certain equilibrium points (or fixed points) around which the molecule moves for a long time. The stability analysis of these points provides an indication of whether or not suspension of the molecule will occur. A dumbbell will be held fixed in the cellular flow if the net force on each bead vanishes. From equations (5) equilibrium points of each bead, located at (x_1, y_1) and (x_2, y_2), must satisfy the following conditions:

$$\begin{aligned} &\sin x_1 \cos y_1 + B(x_2 - x_1) = 0 \qquad && -\sin y_1 \cos x_1 + B(y_2 - y_1) + V_g = 0 \\ &\sin x_2 \cos y_2 - B(x_2 - x_1) = 0 \qquad && -\sin y_2 \cos x_2 - B(y_2 - y_1) + V_g = 0. \end{aligned} \tag{10}$$

In the above equations we have considered that equilibrium is determined by the balance between drag, spring and gravity forces (the Brownian term is neglected).

Due to the fact that solving these transcendental equations is not an easy task, the complete set of fixed points will be found by numerical integration of the system of equations (5) without the Brownian term. We first calculated the trajectories for a large number of dumbbells located at random initial positions in the square $[0, 2\pi] \times [0, 2\pi]$ and then analysed the dynamics in the long-term regime ($t \to \infty$).

In analysing the results we have found that dumbbell dynamics in the long-term regime converges to three different kinds of paths. Indeed, we found that there is a fraction of the dumbbells that moves in open paths along the downdraft region of the flow field, another fraction moves in limit cycles with the two beads of the dumbbell in the same single cell and a fraction of dumbbells remains at fixed points with both beads at rest in different cells of the flow field.

When a dumbbell moves in a limit cycle or an open path the beads remain close to one another and the molecule length, Q, varies in a range generally much smaller than the cell length, π. In contrast, if the molecule is at a fixed point, the molecule length is fixed and takes values that are generally of the order of the cell length, π. Thus, dumbbell trajectories which converge to open or closed paths can be distinguished from those trapped in fixed points because in the first case the dumbbell lengths will cover a continuous range of small separation lengths, whereas in the second case the length remains constant. These statements are easily verified in figures 7(a) and (b) where probability density functions for Q are shown for the long-term behaviour of the ensemble of molecules. For example, in figure 7(b), which was obtained for $B = 0.08$ and $V_g = 0.5$, it can be seen that the distribution has a continuous part at the lowest range of lengths, $Q \ll \pi$, corresponding to molecule lengths which are in open or closed paths. There is also a number of isolated peaks in the range of lengths comparable to the cell size, which correspond to molecules located at fixed points. Similarly, figure 7(a), obtained for $B = 0.03$ and $V_g = 0.5$, shows the same structure with two interesting differences with respect to the preceding case: there is a larger number of peaks and the separation between the continuous part and the discrete part is less pronounced.

Figures 7(a) and (b) show that the number of fixed points decreases as the spring constant increases. The reason for this behaviour is that a dumbbell with a large spring constant is not easy to stretch. Correspondingly, we expect that as B is increased some of the fixed points cease to exist (for large values of B the molecule behaves as a single particle and in this

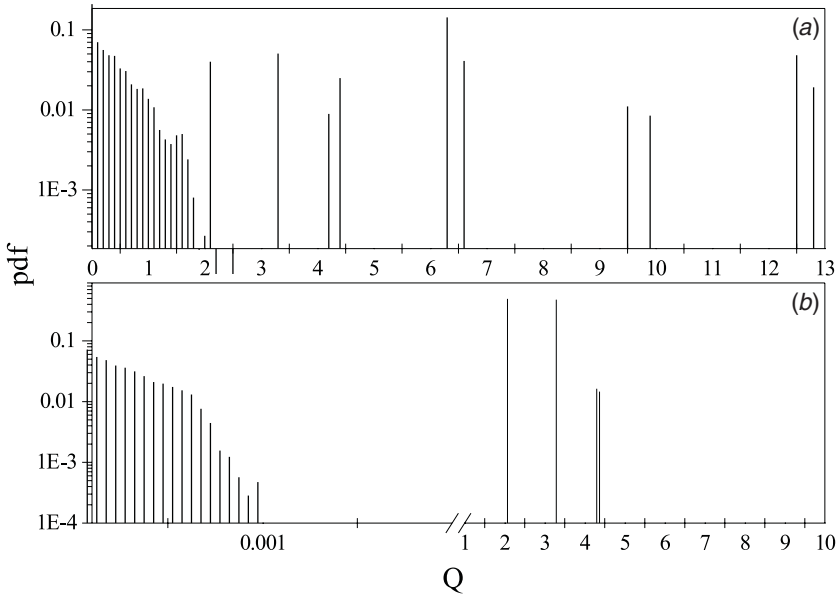

Figure 7. Normalized probability density distribution of molecule lengths, Q, for an ensemble of dumbbells in the long-term regime for $V_g = 0.5$ and $D = 0.01$: (*a*) $B = 0.03$ and (*b*) $B = 0.08$.

situation the only fixed points that occur are those shown in figure 2). Equation (10) shows that the modulus of the product $B\mathbf{Q}$ is limited by the sum of the flow velocity and V_g. Thus, if B is small, Q may take a greater range of values than for large B, that is, the dumbbell may be stretched by the action of the flow field and gravity and, eventually, it will be able to reach the points where the net force on both beads vanishes.

We note that the procedure used to compute the above distributions of lengths produces only stable fixed points. A fixed point of the system obtained from equations (5) is considered stable if the real part of all the eigenvalues evaluated at the fixed point is negative. The possible values of the eigenvalues, λ, are the roots of the quartic polynomial

$$\mu^4 + A_1\mu^2 + A_2 = 0 \tag{11}$$

where

$$\begin{aligned} &\lambda = \mu - B \\ &A_1 = -z_1^2 - z_2^2 + w_1^2 + w_2^2 - 2B^2 \\ &A_2 = z_1^2 z_2^2 + w_1^2 w_2^2 - z_1^2 w_2^2 - w_1^2 z_2^2 + 2B^2(w_1 w_{2-} z_1 z_2) + B^4 \\ &z_i = \cos x_i \cos y_i \\ &w_i = \sin x_i \sin y_i \qquad i = 1, 2. \end{aligned} \tag{12}$$

The roots of the polynomial (11) depend on the coordinates of the beads at the fixed points and in general the problem can only be solved numerically. However, let us now consider a special case for which the fixed point may be easily obtained. Consider the beads of a dumbbell oriented perpendicular to the gravity, at positions (x_1, y_1), (x_2, y_2) in the flow field, such that the following relations hold:

$$\begin{aligned} &x_2 = 2\pi - x_1 \qquad y_1 = y_2 \\ &0 < x_1 < \pi \qquad 0 < y_1 < 2\pi. \end{aligned} \tag{13}$$

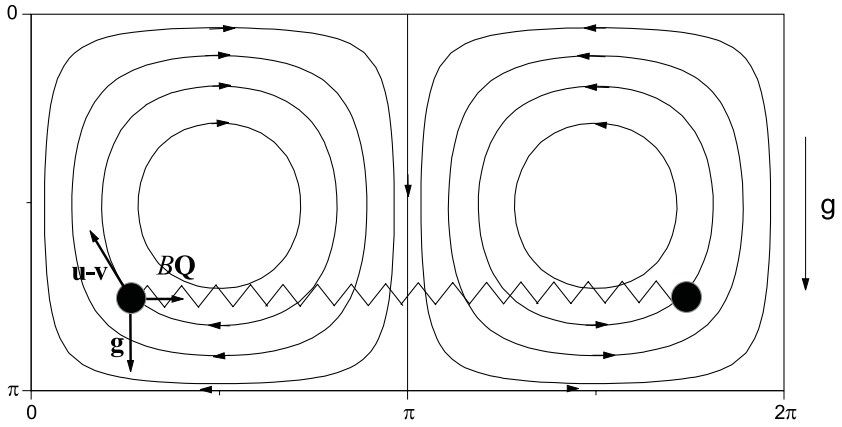

Figure 8. Schematic view of the dumbbell at the equilibrium point defined by $x_2 = 2\pi - x_1$, $y_1 = y_2$; $< x_1 < \pi, 0 < y_1 < 2\pi$. The balance between the drag, spring and gravity forces is indicated by arrows on one of the beads.

A schematic view of the forces acting on one of the beads is shown in figure 8. The other bead is in a symmetrical position with respect to the axis $x = \pi$. The gravity force is directed downwards, the spring force is horizontal and the drag force has components opposed to both the gravity and the spring forces. Under conditions (13) it is expected that an equilibrium of forces is obtained for certain values of B and V_g. Introducing relations (13) in equations (10) we have

$$\sin x_1 \cos y_1 + 2B(\pi - x_1) = 0 \qquad -\cos x_1 \sin y_1 + V_g = 0. \tag{14}$$

It is immediately obtained that the proposed equilibrium point exists only if

$$V_g < 1 \qquad \text{and} \qquad B < 1/\pi. \tag{15}$$

Let us now investigate the stability of this fixed point. To determine the roots of the quartic polynomial given in equation (11), the relations at the equilibrium points (equation (13)) are substituted into the expressions for the coefficients (equation (12)). It is obtained that

$$\lambda = -B \pm \sqrt{(z_1 \pm B)^2 - w_1^2}. \tag{16}$$

Equations (14) together with equation (16) can be used to obtain fixed points and their stability as a function of B. Figure 9 summarizes the results for $V_g = 0.5$. The position of one of the beads is plotted as it varies with B in the single-particle velocity field. As before, the other bead is located in a symmetrical position with respect to the vertical line $x = \pi$. For $B \to 0$ three stable solutions for (x_1, y_1) can be obtained from equations (14): $P_1 = (\cos^{-1} V_g, \pi/2)$, $P_2 = (\pi - \cos^{-1} V_g, 3\pi/2)$ and $P_3 = (0, \sin^{-1} V_g)$. The corresponding molecule lengths, $Q = x_2 - x_1$, are $2(\pi - \cos^{-1} V_g)$, $2\cos^{-1} V_g$ and 2π, respectively. The points P_1 and P_3 evolve with B as indicated by the arrows in figure 9 and they collapse for $B_1 \simeq 0.110$. For $B > B_1$, P_1 and P_3 disappear. The fixed point labelled P_2 is stable from $B = 0$ up to $B_2 \simeq 0.271$, then it becomes unstable. Alternatively, this evolution can be seen in figure 10 where the molecule length of the three fixed points is plotted against the spring constant. The largest real part of the eigenvalues is also plotted. It can be seen that it decreases linearly with B ($\mathrm{Re}(\lambda_{\max}) = -B$) but then it rapidly increases and becomes positive for

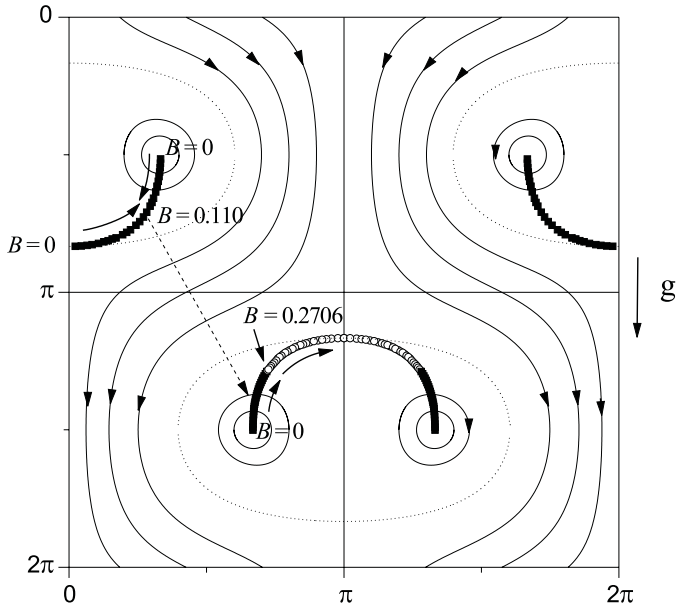

Figure 9. Evolution with B of the fixed point defined by $x_2 = 2\pi - x_1$, $y_1 = y_2$; $0 < x_1 < \pi$, $0 < y_1 < 2\pi$. Superposed streamlines correspond to the velocity field for a sedimenting single particle in the cellular flow field: ■, stable fixed points; ○, unstable fixed points. The collapse between the two stable fixed points on the upper branch occurs at $B = 0.1100$. Transition from a stable to an unstable fixed point in the lower branch occurs at $B = 0.2706$.

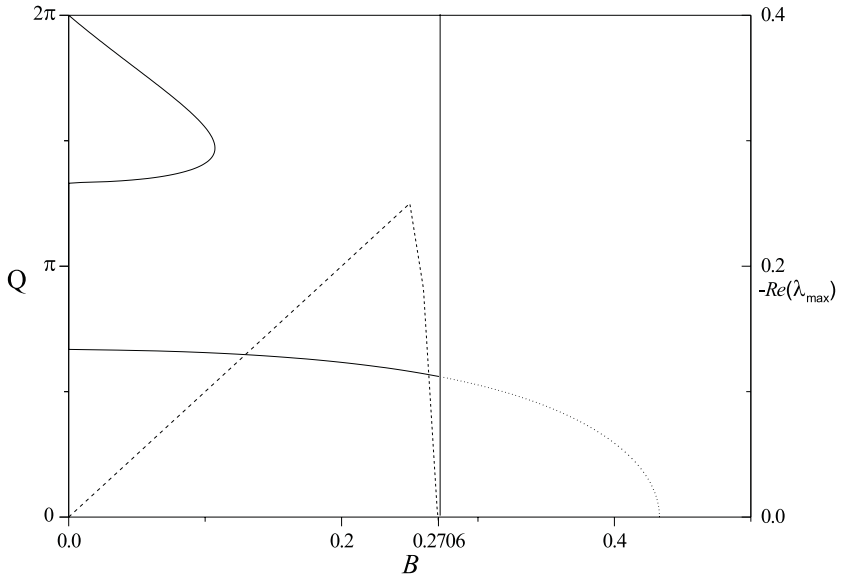

Figure 10. Evolution of the fixed point defined by $x_2 = 2\pi - x_1$, $y_1 = y_2$; $0 < x_1 < \pi$, $0 < y_1 < 2\pi$. Left axis: dumbbell length as a function of B: ——, stable fixed points; - - - -, unstable fixed points. Right axis: · · · · · ·, maximum real part of the eigenvalues, $\mathrm{Re}(\lambda_{\max})$.

$B \simeq 0.271$. In summary, in the range $0 < B < B_2$ there are only stable fixed points. For larger B the molecule cannot be trapped at fixed points of the type defined by equations (14).

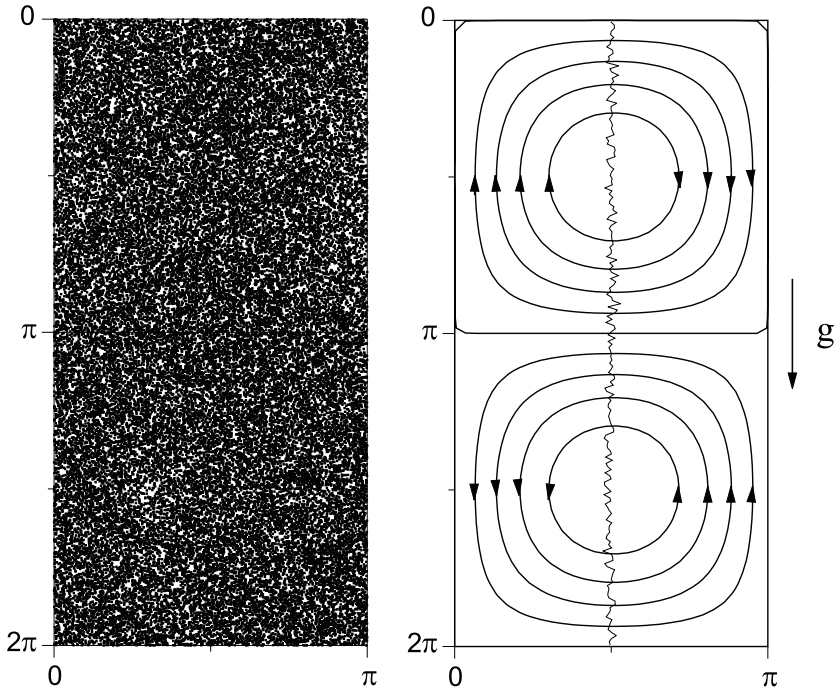

Figure 11. Left-hand side: dumbbell centre of mass position plot obtained by folding the whole path to fit in the rectangle $[0, \pi] \times [0, 2\pi]$. Right-hand side: centre of mass average trajectory and flow streamlines. Note that the average trajectory runs through points of the flow with zero vertical velocity. Parameters are $B = 0.7$, $V_g = 1$ and $D = 0.05$.

Other types of fixed points, where the molecule is not in a horizontal position, admit a similar treatment.

We can now give a picture of what happens with the average settling velocity $\langle V \rangle$ presented in figure 5. First, figures 7 together with the preceding results clearly show that the number of stable fixed points increases as B decreases. A molecule which moves in the vicinity of a given fixed point has a probability of getting trapped, and this probability is measured by the real part of λ_{max} which is equal to $-B$. Thus, while the number of fixed points increases their stability decreases ($\mathrm{Re}(\lambda_{max}) = -B \to 0$). The average settling velocity results are smaller than the still fluid settling velocity because the molecules are delayed when they are in the zone of influence of a fixed point. But if B decreases further, approaching zero, the stability of the fixed points drops and beads may escape more easily, thus the average settling velocity increases again (for $B = 0$ the average settling velocity equals V_g).

Let us now briefly explain the maximum on the average settling velocity for $V_g > 0.5$, presented in figure 6. For $B = 0.7$, the calculated value of $\langle V \rangle$ is similar to V_g and for $B = 0.08$, $\langle V \rangle$ is larger than V_g and equal to the maximum value. Each of the dumbbell trajectories for these two cases is folded to make it fit in the rectangle $[0, \pi] \times [0, 2\pi]$, and the results plotted with dots in figures 11(a) and 12(a). This procedure is useful to visualize in a single pattern of cell the space regions more frequently visited by the dumbbell as it drifts downwards. So, in figure 11(a) it can be seen that the points are uniformly distributed which means that there is no preference for dumbbells to travel through any special region. In contrast, in figure 12(a) some accumulation of points around a sinuous path is observed indicating some preference of the dumbbell to pass near such regions.

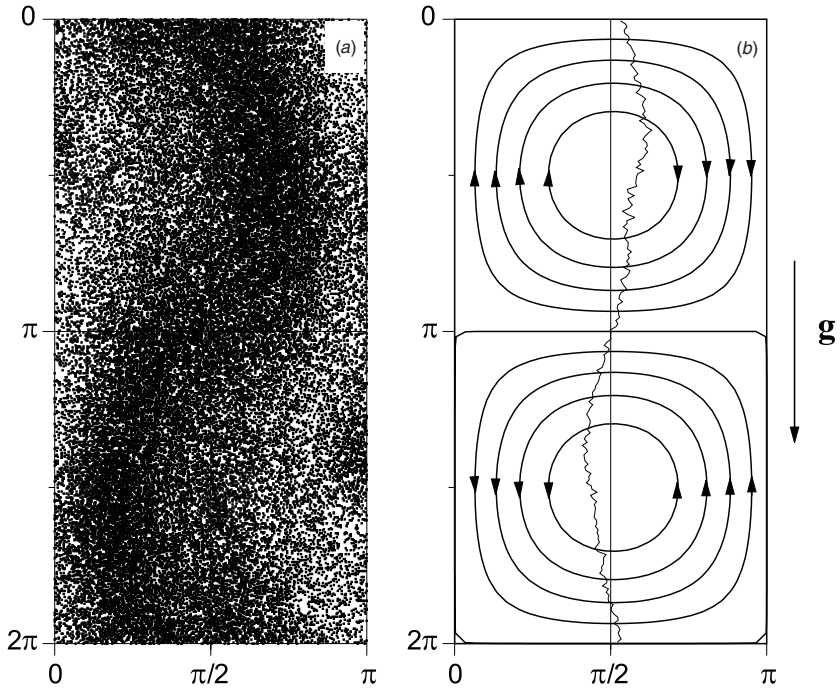

Figure 12. Left-hand side: dumbbell centre of mass position plot obtained by folding the whole path to fit in the rectangle $[0, \pi] \times [0, 2\pi]$. Right-hand side: centre of mass average trajectory. Note that the average trajectory runs through points of the flow with positive vertical velocity. Parameters are $B = 0.08$, $V_g = 1$ and $D = 0.05$.

In figures 11(b) and 12(b), we show the average dumbbell trajectory, $(X(t), \langle Y^* \rangle(t))$, where X is the coordinate of the centre of mass in the horizontal direction and $\langle Y^* \rangle$ is the averaged coordinate of the centre of mass in the vertical direction, calculated as

$$\langle Y^* \rangle = \int_0^\pi Y^* \, \mathrm{dx} \tag{17}$$

where Y^* is the remainder of dividing $Y(t)$ by the flow periodicity, 2π. It can be observed that in the case $B = 0.7$ and $V_g = 1$, the average trajectory approximately corresponds to a vertical line with $X = 3/2\pi$. Thus, the flow field evaluated along the dumbbell trajectory is $u_y(3/2\pi, \langle Y^* \rangle) = 0$ and does not contribute to the dumbbell settling velocity which is equal to V_g. In contrast, it can be seen that the average trajectory for $B = 0.08$ and $V_g = 1$ has a sinuous shape and it explores spatial regions where the flow velocity $u_y(X, \langle Y^* \rangle) > 0$. Thus, in this condition the flow contributes to enhancing the settling process making the dumbbell have an average velocity larger than V_g.

5. Concluding remarks

The results of the preceding section show that the settling motion of a deformable body could be influenced by its internal structure. Such a body was modelled here by the elastic dumbbell consisting of two beads connected by a Hookean spring, a simple model which, in spite of its simplicity, has been successfully used to reproduce several rheological properties of real polymer chains.

Using the elastic dumbbell we have shown that the molecule internal structure, characterized here by the value of the spring constant, produces an overall dynamics which presents phenomena such as hypo- or hypersedimentation, not observed for simple bodies such as spherical particles. It was suggested that these properties are related to the ability of polymers to store internal energy through stretching mechanisms. More precisely, it was stated that stretching is the mechanism which facilitates the existence of fixed points. In this work it was shown that the interaction of a molecule with the convective flow produces a set of stable fixed points at which the molecule can remain trapped for some time. These fixed points cause the average settling velocity to be smaller than that in a fluid at rest. Further, it was found that for certain conditions the molecule is trapped indefinitely and the settling process is interrupted. To further clarify the connection between fixed points and settling velocity, we investigated the fixed points in detail. We found that the number of fixed points depends on the spring constant. Specifically, we found that the number of fixed points decreases, but their stability increases, with the spring constant. Thus, fixed points and their stability together determine the average velocity of the settling molecules. We then focused on one of the fixed points and studied it in detail. We have shown that fixed points disappear for sufficiently large values of V_g. Under this condition, the molecule can no longer get trapped and it is able to settle down. Nevertheless, for low enough spring constants the molecule stretches and the beads can visit regions of downflow velocities where the molecule settles down faster. This phenomenon contributes to increasing the average settling velocity to values larger than V_g.

Acknowledgments

We are grateful to J P Hulin and G Drazer for helpful and stimulating discussions. Also, we thank A L Calvo for encouraging us to pursue this work and M A Aguirre for fruitful suggestions.

References

[1] Smith D E, Babcock H P and Chu S 1999 *Science* **283** 1724
[2] Perkins T, Smith D E and Chu S 1997 *Science* **276** 2016
[3] Tong P, Ye X and Ackerson B J 1997 *Phys. Rev. Lett.* **79** 2363
[4] Ruetsh G R and Meiburg E 1993 *Phys. Fluids* A **5** 10
[5] McLaughlin J B 1989 *Phys. Fluids* A **1** 7
[6] Happel J and Brenner H 1973 *Low Reynolds Number Hydrodynamics* (Leyden: Noordhoff)
[7] Cristanti A, Falcioni M and Vulpiani A 1991 *Riv. Nuovo Cimento* **14** 51
[8] Stommel H 1949 *J. Marine Res.* **8** 24
[9] Maxey M R and Corrsin S 1986 *J. Atmos. Sci.* **43** 1112
[10] Maxey M R 1987 *Phys. Fluids* **30** 7
[11] Bird R B, Hassager O, Armstrong R C and Curtiss C F 1977 *Dynamics of Polymeric Liquids* vol II (New York: Wiley)
[12] Goh C J, Phan-Thien N and Atkinson J D 1984 *J. Chem. Phys.* **81** 6259